INFLUENCE OF SOLAR ACTIVITY VARIATIONS ON INTERDIURNAL VARIABILITY OF *NmE* OBTAINED FROM GROUND-BASED LOW LATITUDE IONOSONDE DATA IN GEOMAGNETICALLY QUIET CONDITIONS

© 2025 A.V. Pavlov*, N. M. Pavlova

Pushkov Institute of Terrestrial Magnetism, Ionosphere, and Radio Wave Propagation RAS (IZMIRAN), Moscow, Troitsk, Russia

**e-mail: pavlov@izmiran.ru*

Received October 30, 2024

Revised March 24, 2025

Accepted April 14, 2025

Abstract. The study of the interdiurnal variations in the statistical characteristics of the electron number density *NmE* of the ionospheric *E* layer peak for each month M of the year in geomagnetically quiet conditions at low and moderate solar activity was carried out based on hourly measurements of the critical frequency of the *E* layer of the Huancayo and Jicamarca ionosondes from 1957 to 1989 and 1998-2006, respectively. The authors have calculated the mathematical expectation NmE_E(UT,M), NmE_A(UT,M) arithmetic mean, the standard deviation σ_E(UT,M) and the variation coefficient CV_E(UT,M) of *NmE*(UT,M) from NmE_E(UT,M), respectively, where UT is the universal time. The calculations showed that the value of CV_E(UT,M) that determines the relative interdiurnal *NmE* variability vary between 4−14% and 3−18% at low and moderate solar activity, respectively. It was found for the first time that the interdiurnal variability of *NmE* can either increase or decrease when solar activity changes from low to moderate levels,. In the first case, the increase in σ_E(UT,M) prevails over the growth of NmE_E(UT,M), in the second case, the growth of NmE_E(UT,M) prevails over the increase in σ_E(UT,M).

Keywords: *Low-latitude ionosphere, E-region, modeling and forecasting*

DOI: 10.31857/S00167940250406e9

1. INTRODUCTION

The reliability of radio-frequency communication systems and global navigation satellite systems depends on attenuation, absorption, reflection and refraction and, consequently, on the variability of propagation characteristics, phase and amplitude of radio waves (see, for example, [Davis, 1973; Brunelli and Namgaladze, 1988]). A number of monographs describe most types of variability of electron concentration $N_{(e)\ of}$ the ionosphere (see, for example, [Brunelli and Namgaladze, 1988]). In recent decades, a large number of studies have been published on the inter-diurnal (day-to-

day or interdiurnal) variability of $N_{(e)}$, where the N_e value measured under geomagnetically quiet conditions over approximately the same point on the Earth's surface at the same or close values of local time, day number of the year, and solar activity level, varies significantly from one day to another day (see, e.g., [Cander, 2019; Liu et al., 2021] and references in these papers). The main sources of inter-day N_e variability and its characteristics depend on altitude, latitude, and solar activity level. Unless the N_e variability is compared for different altitudes, latitudes, and solar activity levels, the inter-day N_e variability is studied separately for each layer of the low- and mid-latitude ionosphere under low, moderate, and high solar activity.

The interday variability of the maximum electron concentration *NmE* of the ionospheric layer *E* and its sources were discussed, for example, by the authors of [Pavlov and Pavlova, 2016; Moore et al., 2006; Nicolls et al., 2012; Liu et al., 2021; Mendillo, 2020; Pavlov and Pavlova, 2024a]. It follows from numerical models of *NmE* that the value of *NmE* depends on the zenith angle of the Sun, the flux F of X-ray and extreme ultraviolet radiation from the Sun, and the temperature T_n and concentrations $N_{(n)\ of}$ the neutral components of the atmosphere [Pavlov and Pavlova, 2015; Pavlov and Pavlova, 2013; Sojka et al., 2014]. At the same time, ignoring the influence of the X-ray flux on *NmE* leads to a mismatch between the calculated and measured *NmE*. To eliminate this discrepancy, [Yonezawa, 1968] adopted an erroneous hypothesis about the influence of vibrationally excited molecular ions on *NmE* and used a fitting effective recombination coefficient of molecular ions. Unfortunately, this approach has been used in a number of studies of the *E* region of the ionosphere (see, e.g., Antonova et al., 1996; Takayanagi and Itikawa, 1970; Keneshea et al., 1970). It should be noted that in the review of the photochemistry of the *E* and *F* regions of the ionosphere [Pavlov, 2012] it was shown that at the heights of the *E* region of the ionosphere the rate of conversion of vibrationally excited molecular ions into vibrationally unexcited molecular ions due to collisions with N_2 and O_2 molecules is much greater than the rate of dissociative recombination of these ions, i.e., at the heights of the *E* region of the ionosphere.i.e., vibrationally excited molecular ions do not affect *NmE* and the interday variability of *NmE*

If the measurement result of some parameter is not unambiguously determined, this parameter can be considered as a random variable, part of the variability of which is a consequence of the inevitable errors of the measurements performed (see, for example, Taylor [1985]). In the study under consideration using data of two ionosondes processed manually by , two sources of daily variability *NmE* due to errors of measurements of the critical frequency *foE* of the ionospheric layer *E* *are* taken into account.

Thus, the considered variability *NmE* is determined by the interday variability F, T_n, N_n, and measurement errors *foE*. At the same time, as stated in [Pavlov and Pavlova, 2024a], the first basic (initial) cause of the interday *variability*, *F*-, T_n-, and N_n-variations of the flux of X-ray and extreme

ultraviolet solar radiation with characteristic times of less than a day, cannot be described using the mean daily index *F10*.7 or other mean daily indices of solar activity.

The second basic cause of the interday variability of T_n and N_n− is incorrect identification of geomagnetically calm conditions when using three-hourly indices of geomagnetic activity [Pavlov and Pavlova, 2024a]. In addition, the interday variability of metal ions existing in the *E* region of the ionosphere and variations of the Sun's zenith angle at changing the number of a day in the year during the month M of the year under consideration at a given value of world time UT apparently also contribute to the interday variability of *NmE* [Pavlov and Pavlova, 2024a].

The analysis of these sources allows us to consider *NmE* as a random parameter, and statistical methods described, for example, in monographs [Ross, 2004; Gatti, 2005] can be applied to study its variations. Following the statistical approach, the mathematical expectation (expected value) NmE_E(UT,M), the arithmetic mean NmE_A(UT,M), the standard deviation σ_E(UT,M) and the coefficient CV_E(UT,M) of *NmE* variation with respect to NmE_E(UT,M) were calculated in [Pavlov and Pavlova, 2024a] under geomagnetically calm conditions using hourly measurements of the critical frequency *foE* of the ionosphere of the mid-latitude Dourbes ionosonde. It is clear from this study that the values of NmE_E, NmE_{MP}, and NmE_{MED} differ significantly, and to best describe a set of observations with a single statistical parameter *NmE*, one should use NmE_E but not NmE_{MP} or NmE_{MED}. Thus, the calculated statistical parameters σ_E(UT,M) and $CV_{(E)}$(UT,M) for the given values of M, UT, geographic coordinates, and solar activity level under geomagnetically calm conditions should be used as absolute and relative variability *NmE*(UT,M).

It should be noted that the interday variability of *NmE* was studied in [Pavlov & Pavlova, 2016] only for low solar activity conditions based on *foE*(UT,M) frequencies measured by the low-latitude Huancayo and Jicamarca ionosondes under geomagnetically calm conditions from 1957 to 2015. The aim of this work is to study for the first time the influence of solar activity variations on the relative inter-day variability of the low-latitude *NmE* by comparing the calculated CV_E(UT,M) coefficients under low and moderate solar activity conditions using *foE*(UT,M) frequencies measured by the Huancayo and Jicamarca low-latitude ionosondes under geomagnetically calm conditions

2. EXPERIMENTAL DATA AND METHOD OF THEIR ANALYSIS

The present work uses hourly measurements of the *foE* frequency of the Huancayo (12.0° S, 284.8° E) and Jicamarca (11.9° S, 283.1° E) ionosondes for the periods 1957− 1989 (Huancayo) and 1998− 2006 (Jicamarca) from the US and UK Solar-Terrestrial Physics World Data Center databases, respectively, obtained by manual processing of ionograms. In this case.

absolute accuracy of *NmE* measurements is 0.05 MHz [Piggot and Raver, 1978], determining an estimate of one of the sources of the interday variability of *NmE*. We use the model [Picone et al., 2002] of thermospheric composition and structure to determine the variations of T_n and N_n and the

algorithm of [Pavlov and Pavlova, 2010] to calculate the variations of the Sun's zenith angle when moving from the geographic coordinates of the Huancayo ionosonde to the geographic coordinates of the Jicamarca ionosonde. It follows from these calculations that the proximity of the geographic coordinates of the Huancayo and Jicamarca ionosondes allows us to neglect the influence of changes in F, T_n, N_n, and the Sun's zenith angle on *NmE* and the corresponding sources of the interday variability of *NmE* at the specified change of these coordinates and a given value of UT. In this approximation, it is possible to use the Jicamarca ionosonde data instead of the missing Huancayo ionosonde data in calculating the statistical characteristics of the *NmE* variability. It should be noted that the Jicamarca ionosonde data are used only for February at moderate solar activity, when the number of Huancayo ionosonde measurements used is not sufficient to determine the statistical parameters of *NmE* (see Section 3). The *NmE* values measured by ionosondes are calculated using the relationship between *NmE* and *foE* (see, for example, [Piggot and Raver, 1978]).

To the best of the authors' knowledge, there are no published estimates of the absolute accuracy of *NmE* measurements using the automated ionogram processing system. It should be noted that the results of *NmE* measurements of the Jicamarca ionosonde obtained using this system and given in the database of the World Solar-Terrestrial Physics Data Center of Great Britain are not used in this work, because it is not clear to what extent the use of these data instead of the data of the manual ionogram processing system can change the absolute accuracy of *NmE* measurements and can affect the interday variability of *NmE*

The solar X-ray and ultraviolet radiation flux, which ionizes the neutral components of the thermosphere and forms the *NmE* of middle and low latitudes, is approximated in terms of changes in the indices *F10*.7 (mean daily solar radiation flux at a wavelength of 10.7 cm for the days under consideration) and <*F10*.7> (arithmetic mean of the *F10*.7 index for 81 days centered on the day under consideration) according to an empirical model [Richards et al, 1994]. The *NmE* value also depends on the temperature and concentrations of the main neutral components of the thermosphere, for the determination of which the solar activity indices *F10*.7, <*F10*.7> and *F10*.7p (the value of *F10*.7 for the preceding day) and 3-hour *Ap* indices of geomagnetic activity are used in the generally accepted international empirical model of the thermosphere structure [Hedin, 1987; Picone et al., 2002]. The connection of the 3-hour *Ap* and *Kp* indices of geomagnetic activity is known [Akasofu and Chapman, 1972], and the *Kp* index can be used instead of the *Ap* index for identification of geomagnetically quiet conditions.

The calculations performed used *foE* measurements at times when each of the indices *F10*.7, *F10*.7p, and <*F10*.7> varied between 65− 85 sfu (1 sfu= 10^{-22} W m^{-2} $Hz^{-1)}$ at low solar activity and 85− 125 sfu− at moderate solar activity, and the three-hour geomagnetic activity index *Kp* did not

exceed 3 during the 24-hour period preceding the time of *foE* measurement and at the time of *foE* measurement (geomagnetically calm conditions).

The results of *foE* measurements are sorted for each month of the year for geomagnetically quiet conditions separately at low and moderate solar activity at each of the time moments UT = 12, ..., 22 h, fixing the data samples used. The relationship between local solar time SLT and UT is defined by the relationship SLT= UT +λ /15, where λ− is geographic longitude in degrees, and the units of SLT and UT− are hours. Most of the data used are obtained by the Huancayo ionosonde and the longitude of this ionosonde is used in determining SLT. As a result, the UT = values of 12, 13, ... , 22 h correspond to SLT= 06:59, 07:59, ..., ..., 16:59. It should be kept in mind that at nighttime the *NmE* values are too small at low latitudes and are not detected by the ionosonde [Titheridge, 2001; 2003]. That is why data at UT< 12 h are excluded from the analysis, since these data are either missing (night conditions) or the number of these data in the sample is less than 30, in which case it is impossible to correctly determine the statistical parameters [Gatti, 2005; Verma and Verma, 2020].

The considered statistical parameters *NmE* are determined according to the method given in [Pavlov and Pavlova, 2024a]. The relative frequency of an event is taken as the probability (probability distribution density) of the event (see, e.g., Baldin et al., 2016; Ross, 2004; Gatti, 2005), i.e., the probability $W_{(k)}$(UT,M) of the measurement NmE_k(UT,M) is calculated by the formula

$$W_k(\mathrm{UT,M}) = F_k(\mathrm{UT,M})/F(\mathrm{UT,M}), \quad (1)$$

where k is a positive integer; F_k(UT,M) is the number of geomagnetically quiescent NmE_k measurements for selected UT and M; $F(\mathrm{UT,M}) = \sum_{k>0} F_{(k)}(\mathrm{UT,M})$ is the total number of geomagnetically quiescent *NmE* measurements at fixed UT and M.

To determine the percentage probability P_k(UT,M) of measuring $NmE_{(k)}$(UT,M), the following expression is used

$$P_k(\mathrm{UT,M}) = 100 W_k(\mathrm{UT,M}). \quad (2)$$

Mathematical expectation and arithmetic mean value of *NmE* are determined by the formulas

$$NmE_E(\mathrm{UT,M}) = \sum_{k>0} NmE_{(k)}(\mathrm{UT,M}) W_{(k)}(\mathrm{UT,M}), \quad (3)$$

$$NmE_A(\mathrm{UT,M}) = \sum_{k>0} NmE_{(k)}(\mathrm{UT,M})/F(\mathrm{UT,M}). \quad (4)$$

Expressions are used to determine the standard deviation σ_E of *NmE* from NmE_E and the CV_E coefficient of variation of *NmE* relative to $NmE_{(E)}$ expressed as a percentage:

$$\sigma_E(\mathrm{UT,M}) \{= \sum_{k>0} W_{(k)}(\mathrm{UT,M})[NmE_k(\mathrm{UT,M} > -< NmE(\mathrm{UT,M})>]^2\}^{0.5}, \quad (5)$$

CV_E(UT,M)= 100σ_E(UT,M)/$NmE_{(E)}$(UT,M).

(6)

The effect of changes in the level of solar activity on the studied inter-day variability *NmE* is determined by the formula

$$\Delta CV_E(\text{UT,M}) = CV_E^{AV}(\text{UT,M}) - CV_E^{L}(\text{UT,M}), \quad (7)$$

where CV_E^{AV} (UT,M) and CV_E^{L} (UT,M) are coefficients of variation *NmE*(UT,M) relative to NmE_E(UT,M) for moderate and low solar activity conditions, respectively.

The results of *NmE*(UT,M) measurements may sometimes differ greatly from the average values of *NmE*(UT,M), and it is necessary to make sure that these results are not gross measurement errors. The classification of measurement errors is described in many monographs on mathematical statistics, error theory, and measurement processing (see, e.g., [Kobzar, 2006; Seidel, 2022; Durivage, 2022]). Gross measurement errors (outliers, outliers, abnormally large or abnormally small values compared to the mean value of the sample parameter under study) are usually caused by incorrect readings on the instrument scale, operator error in recording observations, malfunction of measuring instruments, or violation of experimental conditions. These errors affect the reliability of measurements and values of the considered statistical parameters, and such measurement errors *NmE*(UT,M) should be detected and excluded from data processing. There are many methods for detecting gross errors, but many of them are limited by the assumption of a Gaussian (normal) probability distribution [David, 1970; Kobzar, 2006]. Often the probability distribution is unknown or the distribution is not Gaussian, as in this study (see Section 4.1). In this case, a method based on Chebyshev's inequality [Durivage, 2022] can be used to identify and remove erroneous values of *NmE*(UT,M). According to Chebyshev's inequality, any sample value of *NmE* cannot deviate from the mathematical expectation of *NmE* by an arbitrary amount (see, e.g., [Durivage, 1979; Kobzar, 2006]:

$NmE_{(E)}$(UT,M) d−≤ *NmE*(UT,M)≤ NmE_E(UT,M)+d, (4)

where d =σ_E(UT,M)(1− $^{q)-0.5}$; q is the confidence level.

If the distribution law of the random variable *X is* normal (Gaussian), the probability of *X* falling into the interval (X_E− 3σ , X_E + 3σ) is 0.997, where X_E is the mathematical expectation of *X* andσ is the standard deviation of *X* from X_E (see, for example, [Baldin et al., 2016]). If the distribution law of *X* differs from the normal distribution (see Section 4.1), the probability of this event will be at least 8/9 [Baldin et al., 2016]. Based on this, the present paper uses the value q= 0.997. The given confidence probability and the calculated values of NmE_E andσ_E allow us to adjust the sample size using inequality (4). Note that the application of the method of successive

approximations in the calculations of statistical parameters *NmE* is conditioned by the dependence of the sample size on NmE_E and σ_E. In the first approximation, condition (4) is not used.

To the authors' knowledge, the Chebyshev inequality has been used in ionospheric studies only in [Pavlov and Pavlova 2024a, b]

3. RESULTS AND THEIR DISCUSSION

Let F(UT,M) be the number of measurements NmE(UT,M) at fixed UT and M (sample size). To determine the values of $NmE_{(E)}$(UT,M), σ_E(UT,M), and $CV_{(E)}$(UT,M), the minimum value of F(UT,M) must be around 30 or greater than 30 [Gatti, 2005; Verma and Verma, 2020]. If only the *NmE* measurements by the Huancayo ionosonde are used, it follows from the calculations that F(UT,M)≥ 64 under low solar activity conditions. As shown in Table 1, the condition F(UT,M)≥ 30 is not fulfilled for M= 2 under moderate solar activity. In this case, the calculated *NmE* statistical parameters cannot be recognized at M= 2. To increase the size of this data sample, the Huancayo and Jicamarca ionosonde measurements under moderate solar activity at M= 2 are used in the calculations. In this case, F(UT,M)≥ 31. Thus, the values of F(UT,M) used are large enough to fulfill the law of large numbers and correctly calculate the considered statistical parameters *NmE*. The statistical study showed that at fixed time and month of the year, the values of $NmE_{(A)}$(UT,M) and $NmE_{(E)}$(UT,M) differ by no more than 0.4% and 5.3% at low and moderate solar activity, respectively, confirming that the sampled data sets used are free from uncorrected values or the influence of these values on the statistical parameters is insignificant.

Table 1.

3.1 Examples of dependence of the probability of occurrence of geomagnetically calm NmE on the month of the year

The calculated month-of-year dependence of the probability P_k(UT,M) of the occurrence of geomagnetically calm *NmEs* around noon at 17:00 UT (11:59 SLT) is presented in percent in Fig. 1 and Fig. 2 under low and moderate activity conditions, respectively. The solid and dashed curves correspond to January and February (upper left panels), March and April (middle left panels), May and June (lower left panels), July and August (upper right panels), September and October (middle right panels), and November and December (lower right panels). Figures 1 and 2 show that the computed probability reaches several local maxima, i.e., the probability distribution is polymodal (multimodal). The polymodality of the distribution indicates significant heterogeneity of the set of values of the quantity under study and may show that the observations consist of several subsets of data with different probability distributions [Titterington et al., 1985; Howell, 2013].

Based on this, we can conclude that the polymodality of P(UT,M) arises due to the existence of several sources of inter-day variability of *NmE*, which have been discussed, for example, by the authors of

[Pavlov and Pavlova, 2016; Moore et al., 2006; Nicholls et al., 2012; Liu et al., 2021; Mendillo, 2020; Pavlov and Pavlova, 2024a]

Figure 1.

Figure 2.

3.2 Dependence of CV_E(UT,M) on the month of the year

In Fig. 3 and Fig. 4 show the calculated dependence on the month of the year of the relative variability of *NmE* at low and moderate solar activity, respectively. From the computational results, the CV_E(UT,M) coefficient varies from 4.3% at time 07:59 SLT in October to 14.0% at 16:59 SLT in March under low solar activity and from 3.1% (10:59 SLT, February) to 17.6% (16:59 SLT, November) under moderate solar activity.

Figure 3.

Figure 4.

The found values of CV_E(UT,M) allow us to determine arithmetically the average *CV* coefficient $^{0}_{E}$ (M) of the variations of *NmE* with respect to NmE_E:

$$CV^{0}_{E}\ (\mathrm{M}) = \frac{1}{11}\sum_{k=12}^{22} CV_E\,(k,\mathrm{M}), \qquad (5)$$

where *k*= UT.

Calculations showed that CV^{0}_{E} (M)= 7, 8, 7, 6, 7, 7, 7, 7, 7, 6, 8, 8, 8, 8% for low solar activity and CV^{0}_{E} (M)= 7, 7, 7, 10, 8, 8, 7, 6, 8, 8, 7, 12, 8, 8, 8, 8, 7% moderate solar activity, where M varies from 1 to 12, respectively. Thus, arithmetically, the arithmetic mean relative inter-day variability of *NmE* does not change significantly with changing the month of the year

3.3 Influence of transition from low to moderate solar activity on the relative inter-day variability of NmE

Expression (1) determines the effect of the investigated change in the solar activity level on the investigated inter-day variability *NmE* by calculating the parameter$\Delta\ CV_E$(UT,M). The time variation of this parameter is shown in Fig. 5 for each month of the year. It can be concluded that the considered increase in the solar activity level increases or decreases the relative inter-day variability of *NmE* in the interval of variation of the parameter $\Delta\ CV_E$(UT,M) from -6.1% (16:59 SLT, February) to 11.2% (9:59 SLT, March).

If we take into account the explicit form CV_E(UT,M) presented, for example, in [Pavlov and Pavlova, 2024a, b], then expression (1) can be transformed to the form:

$$\Delta\ CV_E(\mathrm{UT,M}) = CV^{L}_{E}\ (\mathrm{UT,M})[R_2(\mathrm{UT,M})/R_{(1)}(\mathrm{UT,M}) - 1], \qquad (6)$$

R_1(UT,M)= NmE_E^{AV} (UT,M)/NmE_E^{L} (UT,M), (7)

R_2(UT,M) =σ_E^{AV} (UT,M)/σ_E^{L} (UT,M), (8)

NmE_E^{L} (UT,M) andσ_E^{L} (UT,M) are the mathematical expectation of *NmE*(UT,M) and the standard deviation of *NmE*(UT,M) from NmE_E^{L} (UT,M) at low solar activity; NmE $_E^{AV}$ (UT,M) andσ_E^{AV} (UT,M) are (see, e.g., [Baldin et al., 2016]) at moderate solar activity, respectively.

The calculated time variations of the parameters R_1(UT,M) and R_2(UT,M) for each month of the year are shown in Fig. 6 and Fig. 7 for each month of the year by solid and dashed curves, respectively. The calculations show that 1.07≤ $_{R(1)}$(UT,M)≤ 1.21, 0.62≤ R_2(UT,M)≤ 3.70. The parameters $R_{(1)}$(UT,M) and R_2(UT,M) determine the investigated effect of changing solar activity level on $NmE_{(E)}$(UT,M)andσ_E(UT,M), respectively. If R_2(UT,M)> R_1(UT,M), thenΔCV_E(UT,M)> 0, and an increase in solar activity increases the relative inter-day variability *NmE*. When the condition $_{R(2)}$(UT,M)< R_1(UT,M) is met, *the*ΔCV_E(UT,M)< value is 0, and increasing solar activity decreases the relative inter-day variability of NmE

Figure 5.

Figure 6.

Figure 7.

5. CONCLUSION

The study of daily variations of statistical characteristics of the relative interday variability of electron concentration *NmE* of the maximum of the ionospheric *E* layer for each month of the year in geomagnetically quiet conditions under low and moderate solar activity based on the data of hourly measurements of the critical frequency of the ionospheric *E* layer for the periods was carried out 1957− 1989 and 1998− 2006 from hourly (UT= 12, 13, ..., 22 h) measurements of the Huancayo and Jicamarca ionosondes, respectively. The mathematical expectation NmE_E(UT,M), arithmetic mean NmE_A(UT,M), standard deviationσ_E(UT,M), and coefficient of variation CV_E(UT,M)of *NmE*(UT,M)from $NmE_{(E)}$(UT,M) were calculated, respectively.

From the statistical study, it is observed that the relative difference between $NmE_{(A)}$(UT,M) and $NmE_{(E)}$(UT,M) does not exceed 0.4% and 5.3% for low and moderate solar activity conditions, respectively. From the calculation results, it is found that the CV_E(UT,M) varies between 4− 14% and 3− 18% for low and moderate solar activity, respectively. It is found that the arithmetic mean relative inter-day variability *NmE* varies insignificantly when the month of the year changes or solar activity increases from low to moderate level.

The increase in solar activity level considered in this paper increases or decreases the relative inter-day variability of *NmE* from -6% (16:59 SLT, February) to 12% (15:59 SLT,

September). It is found that when solar activity changes from low to moderate levels, the predominance of an increase in $NmE_{(E)}$(UT,M) over an increase in $\sigma_{(E)}$(UT,M) causes a decrease in the relative inter-day variability of *NmE*, while the predominance of an increase in σ_{E}(UT,M) over an increase in $NmE_{(E)}$(UT,M) causes an increase in the relative inter-day variability of *NmE*.

The results obtained in the present work can be used in the development of probabilistic-statistical models of the ionosphere, the necessity and principles of construction of which are described by the authors of [Kozlov et al., 2014; Becker, 2018; Hunt et al., 2000].

REFERENCES

1. *Akasofu S.-I., Chapman S.* Solar-terrestrial physics. Part 2. M.: Mir, 510 p. 1972.
2. *Antonova L.A., Ivanov-Kholodny G.S., Chertoprud V.E.* Aeronomy of layer *E* (accounting of variations of
UV radiation of the Sun and geomagnetic disturbances). Moscow: Janus, 196 c. 1996.
3. *Baldin K.V., Bashlykov V.N., Rukosuev A.V.* Fundamentals of the theory of probabilities and mathematical
Statisticians. Moscow: FLINTA, 489 p. 2016.
4. *Becker S.A.* Probabilistic-statistical models of the lower unperturbed
of the middle-latitude ionosphere verified from the data of ground-based radiophysical measurements. Avtoref. dissertation of Candidate of Physical and Mathematical Sciences. Moscow: izd-vo IDG RAS, 26 p. 2018.
5. *Brunelli B.E.*, *Namgaladze A.A.* Physics of the ionosphere. Moscow: Nauka, 527 p. 1988.
6. *David G.* Order statistics. Moscow: Nauka, 336 p. 1979.
7. *Davis K.* Radio waves in the ionosphere. M.: Mir, 502 p. 1973.
8. *Seidel A.H.* Errors of measurements of physical quantities. SPb.: Lan, 112 p. 2022.
9. *Kozlov S.I., Lyakhov A.N., Bekker S.Z.* Basic principles of construction of the probabilistic and Statistical models of ionosphere for solving problems of radio wave propagation // Geomagnetism and Aeronomy. T. 54. № 6. C. 767-779. 2014. https://doi.org/10.7868/S0016794014060121
10. *Kobzar A.I.* Applied mathematical statistics. For engineers and scientific
workers. Moscow: Fizmatlit, 816 p. 2006.
11. *Pavlov A.V., Pavlova N.M.* Influence of solar radiation refraction on zenith angle and Sunrise and sunset times in the atmosphere // Geomagnetism and Aeronomy. T. 50. № 2. C. 228-233. 2010.
12. *Pavlov A.V., Pavlova N.M.* Comparison of the measured and calculated by the Moscow ionosonde

electron concentrations of the ionospheric *E* layer maximum in spring conditions // Geomagnetism and Aeronomy. T. 55. № 2. C. 247-257. 2015.
https://doi.org/10.7868/S0016794015020145
13. *Pavlov A.V., Pavlova N.M.* Dependences on the month of the year of statistical characteristics of middle and low latitudes in the daytime geomagnetically calm conditions at low solar activity // Geomagnetism and Aeronomy. T. 56. № 4. C. 431-436. 2016.
https://doi.org/10.7868/S0016794016040167
14. *Piggot V.P., Raver K.* URSI Manual on interpretation and processing of ionograms. M. Science, 342 pp. 1978.
15. *Taylor J.* Introduction to the Theory of Errors. Moscow: Mir, 272 p. 1985.
16. *Cander L.R.* Ionospheric variability / Ionospheric Space Weather. Ed. L.R. Cander. Cham, Switzerland: Springer. P. 59-93. 2019. https://doi.org/10.1007/978-3-319-99331-7_4
17. *David H.A.* Order Statistics. NY and London: John Wiley & Sons, 272 p. 1970.
18. Durivage M.A. Practical Engineering, Process, and Reliability Statistics. Milwaukee, WI: ASQ Quality Press, 356 p. 2022
19. *Gatti P.L.* Probability Theory and Mathematical Statistics for Engineers. London and NY: Spon Press of Taylor & Francis Group, 369 p. 2005. https://doi.org/10.1201/9781482267761
20. *Hunt S.M., Close S., Coster A.J., Stevens E., Schuett L.M., Vardaro A.*. Equatorial atmospheric and ionospheric modeling at Kwajalein missile range // Lincoln Laboratory Journal. V. 12. № 1. P. 45-64. 2000
21. *Hedin A.E.* MSIS-86 thermospheric model // J. Geophys. Geophys. Res. - Space. V. 92. № 5. P. 4649 -4662. 1987. https://dx.doi.org/10.1029/JA092iA05p04649
22. *Howell D.C.* Statistical Methods for Psychology. Belmont, CA: Wadsworth Cengage Learning, 792 p. 2013.
23. *Keneshea T.J., Narcisi R.S., Swider W.* Diurnal model of the E region // J. Geophys. Geophys. Res. V. 75.
N 2. P. 845 - 854. 1970. https://doi.org/10.1029/JA075i004p00845
24. *Liu H., Yamazaki J., Lei J.* Day-to-day variability of the thermosphere and ionosphere / Upper Atmosphere Dynamics and Energetics / Space Physics and Aeronomy Collection, Geophysical Monograph Series 261. V. 4. Eds. W. Wang, Y. Zhang, L.J. Paxton. Hoboken, NY: Wiley. P. 275-300. 2021. https://doi.org/10.1002/9781119815631.ch15
25. *Mendillo M.* Day-to-day variability of the ionosphere / The Dynamical Ionosphere: A Systems Approach to Ionospheric Irregularity. Eds. M. Materassi, B. Forte, A.J. Coster, S. Skone. Coster, S. Skone. Amsterdam: Elsevier. P. 7-11. 2020. https://doi.org/10.1016/B978-0-12-814782-5.00002-9

26. *Moore L., Mendillo M., Martinis C., Bailey S.* Day-to-day variability of the *E* layer // J. Geophys. Geophys. Res. - Space. V. 111. № 6. ID A06307. 2006. https://doi.org/10.1029/2005JA011448
27. *Nicolls M.J., Rodrigues F.S., Bust G.S.* Global observations of *E* region plasma density morphology and variability // J. Geophys. Geophys. Res. - Space. V. 117. № 1. ID A01305. 2012. https://doi.org/10.1029/2011JA017069
28. *Pavlov A.V.* Ion chemistry of the ionosphere at *E*- and F-region altitudes: A review // Surv. Geophys. V. 33. № 5. P. 1133-1172. 2012. https://doi.org/10.1007/s10712-012-9189-8
29. *Pavlov A.V., Pavlova N.M.* Comparison of *NmE* measured by the Boulder ionosonde with model predictions near the spring equinox // J. *Atmos*. Atmos. Sol.-Terr. Phy. V. 102. P. 39-47. 2013. https://doi.
30. *Pavlov A.V., Pavlova N.M.* Influence of solar activity variations on interdiurnal variability of *NmE* in geomagnetically quiet conditions obtained from ground-based Dourbes // Geomagn. Aeronomy. V. 64. № 3. P. 376-390. 2024a. https://doi.org/10.1134/S0016793224600139
31. *Pavlov A.V., Pavlova N.M.* Impact of the solar activity variations on the low-latitude day-to-day variability of *NmF2* during geomagnetically quiet conditions obtained from the Huancayo and Jicamarca ionosonde observations // Pure Appl. Geophys. V. 181. № 7. P. 2177-2195. 2024b. https://doi.org/10.1007/s00024-024-03503-2
32. *Picone J.M., Hedin A.E., Drob D.P., Aikin A.C.* NRLMSISE-00 empirical model of the atmosphere: Statistical comparisons and scientific issues // J. Geophys. Geophys. Res. - Space. V. 107. № 12. ID 1468. 2002. https://doi.org/10.1029/2002JA009430
33. *Richards P.G., Fennelly J.A., Torr D.G.* EUVAC: A solar EUV flux model for aeronomic calculations // J. Geophys. Geophys. Res. - Space. V. 99. № 5. P. 8981-8992. 1994. https://doi.org/10.1029/94JA00518
34. *Ross S.M.* Introduction to Probability and Statistics for Engineers and Scientists. Amsterdam: Elsevier Academic Press, 624 p. 2004.
35. *Sojka J.J., Jensen J.B., David M., Schunk R.W., Woods T., Eparvier F., Sulzer M.P., Gonzalez S.A., Eccles J.V.* Ionospheric model-observation comparisons: *E* layer at Arecibo Incorporation of SDO-EVE solar irradiances // J. Geophys. Geophys. Res. - Space. V. 119. № 5. P. 3844-3856. 2014. https://doi.org/10.1002/2013JA019528
36. *Takayanagi K., Itikawa Y.* Elementary processes involving electrons in the ionosphere // Space Sci. Rev. V. 11. № 23. P. 380– 450. 1970. https://doi.org/10.1007/BF00241527
37. *Titheridge J.E.* Production of the low-latitude night *E* layer // J. Geophys. Geophys. Res. - Space. V. 106. № 7. P. 12781-12786. 2001. https://doi.org/10.1029/2000JA900145

38. *Titheridge J.E.* Ionization below the night *F2* layer - A global model // J. Atmos. Atmos. Sol.-Terr. Phy. V. 65. № 9. P. 1035-1052. 2003. https://doi.org/10.1016/S1364-6826(03)00136-6
39. *Titterington D.M., Smith A.F.M., Makov U.E.* Statistical Analysis of Finite Mixture Distributions. Chichester, UK: John Wiley & Sons, 258 p. 1985.
40. *Verma J.P., Verma P.* Determining Sample Size and Power in Research Studies. Singapore: Springer, 127 p. 2020.
41. *Yonezawa T.* A consideration of the effective recombination coefficient in the *E-region of* the ionosphere // J. Atmos. Atmos. Terr. Phys. V. 30. № 10. P. 473-478. 1968. https://doi.org/10.1016/0021-9169(68)90120-7

Table 1. Total number of *NmE*(UT,M) concentrations used to calculate *NmE*(UT,M) statistical parameters from Huancayo ionosonde data at moderate solar activity after applying Chebyshev's inequality

UT	M											
	1	2	3	4	5	6	7	8	9	10	11	12
12:00	60	29	48	66	111	113	65	65	56	72	74	64
13:00	58	25	50	69	116	112	65	65	60	68	72	61
14:00	58	25	51	67	115	116	66	71	62	72	71	64
15:00	57	22	42	55	108	108	62	65	56	61	51	56
16:00	54	19	38	54	96	105	59	60	44	49	43	59
17:00	57	21	41	57	100	109	62	67	39	50	44	56
18:00	55	16	38	61	108	105	60	68	40	47	47	52
19:00	54	20	41	63	115	114	58	69	58	57	57	57
20:00	56	20	45	62	115	114	61	72	67	66	70	53
21:00	52	19	46	67	115	110	59	73	65	60	70	47
22:00	51	19	46	66	113	105	57	69	59	61	62	47

Figure captions

Figure 1. Percentage dependence of the *NmE* probability *P*(UT,M) for low solar activity conditions at 17:00 UT (11:59 SLT). The solid and dashed curves correspond to January and February (upper left panels), March and April (middle left panels), May and June (lower left panels), July and August (upper right panels), September and October (middle right panels), and November and December (lower right panels).

Figure 2. Percentage dependence on the *NmE* probability *P*(UT,M) for conditions of moderate solar activity at 17:00 UT (11:59 SLT). The curve designations are the same as in Fig. 1.

Figure 3. Dependence of the CV_E(UT,M) coefficient on the month of the year for low solar activity conditions at 06:59, 07:59, and 08:59 SLT (solid, dashed, and dotted curves in the upper left panel, respectively); 09:59, 10:59, and 11:59 SLT (solid, dashed and dotted curves in the lower left panel, respectively); 12:59, 13:59 and 14:59 SLT (solid, dashed and dotted curves in the upper right panel, respectively); 15:59 and 16:59 SLT (solid and dashed curves in the lower right panel, respectively).

Figure 4. Dependence of the coefficient CV_E(UT,M) on the month of the year for conditions of moderate solar activity. The curve designations are the same as in Fig. 3.

Figure 5. Time dependence of the parameterΔ CV_E(UT,M) for each month of the year.

Figure 6. Time dependence of the parameters R_1(UT,M) and R_2(UT,M) from January to June. Solid and dashed curves correspond to R_1(UT,M) and R_2(UT,M).

Figure 7. Time dependence of the parameters R_1(UT,M) and R_2(UT,M) from July to December. Solid and dashed curves correspond to R_1(UT,M) and R_2(UT,M).

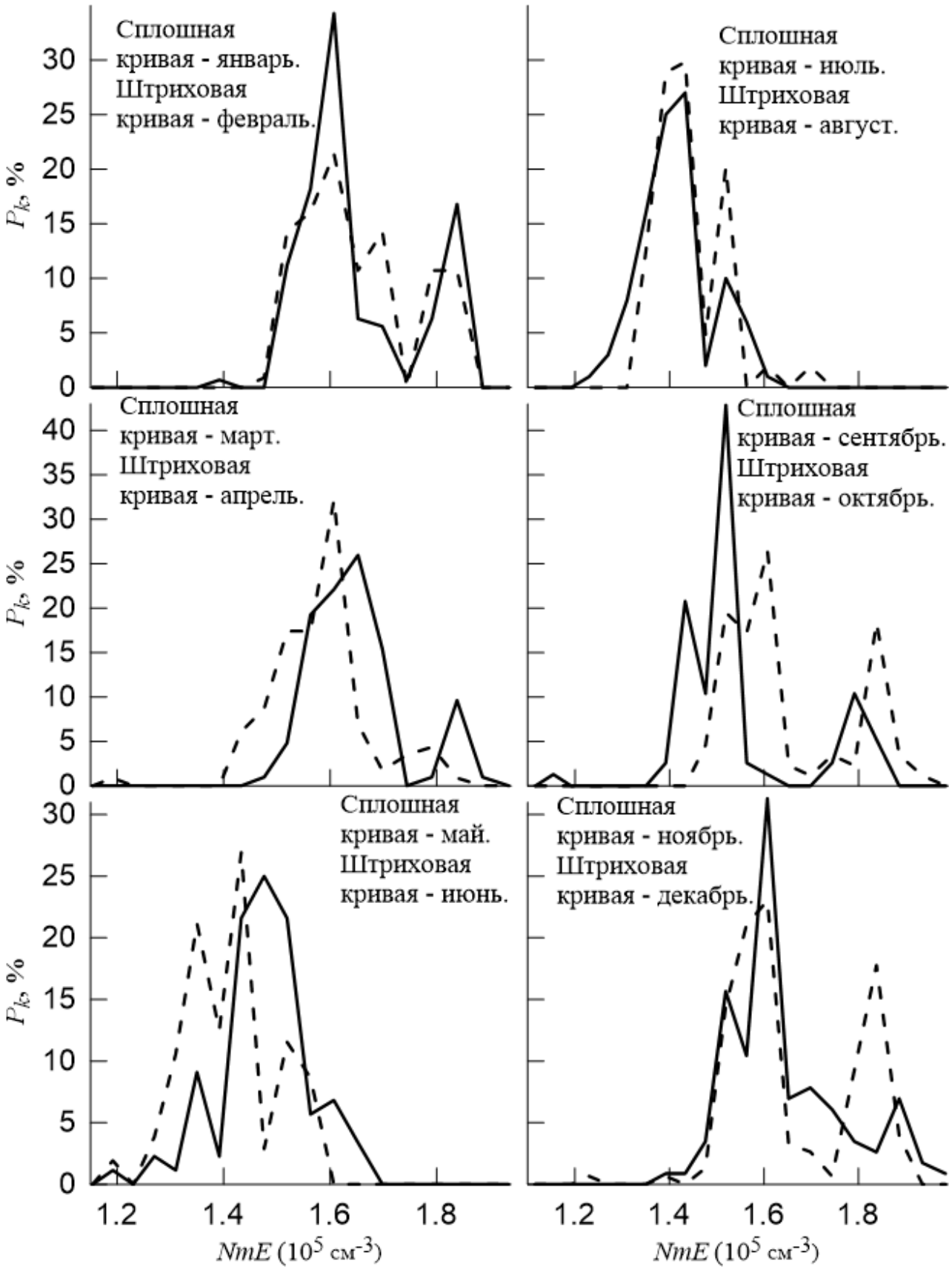
Сплошная кривая - январь. Штриховая кривая - февраль.
Сплошная кривая - июль. Штриховая кривая - август.
Сплошная кривая - март. Штриховая кривая - апрель.
Сплошная кривая - сентябрь. Штриховая кривая - октябрь.
Сплошная кривая - май. Штриховая кривая - июнь.
Сплошная кривая - ноябрь. Штриховая кривая - декабрь.
P_k, %
NmE (10^5 см$^{-3}$)

Figure 1

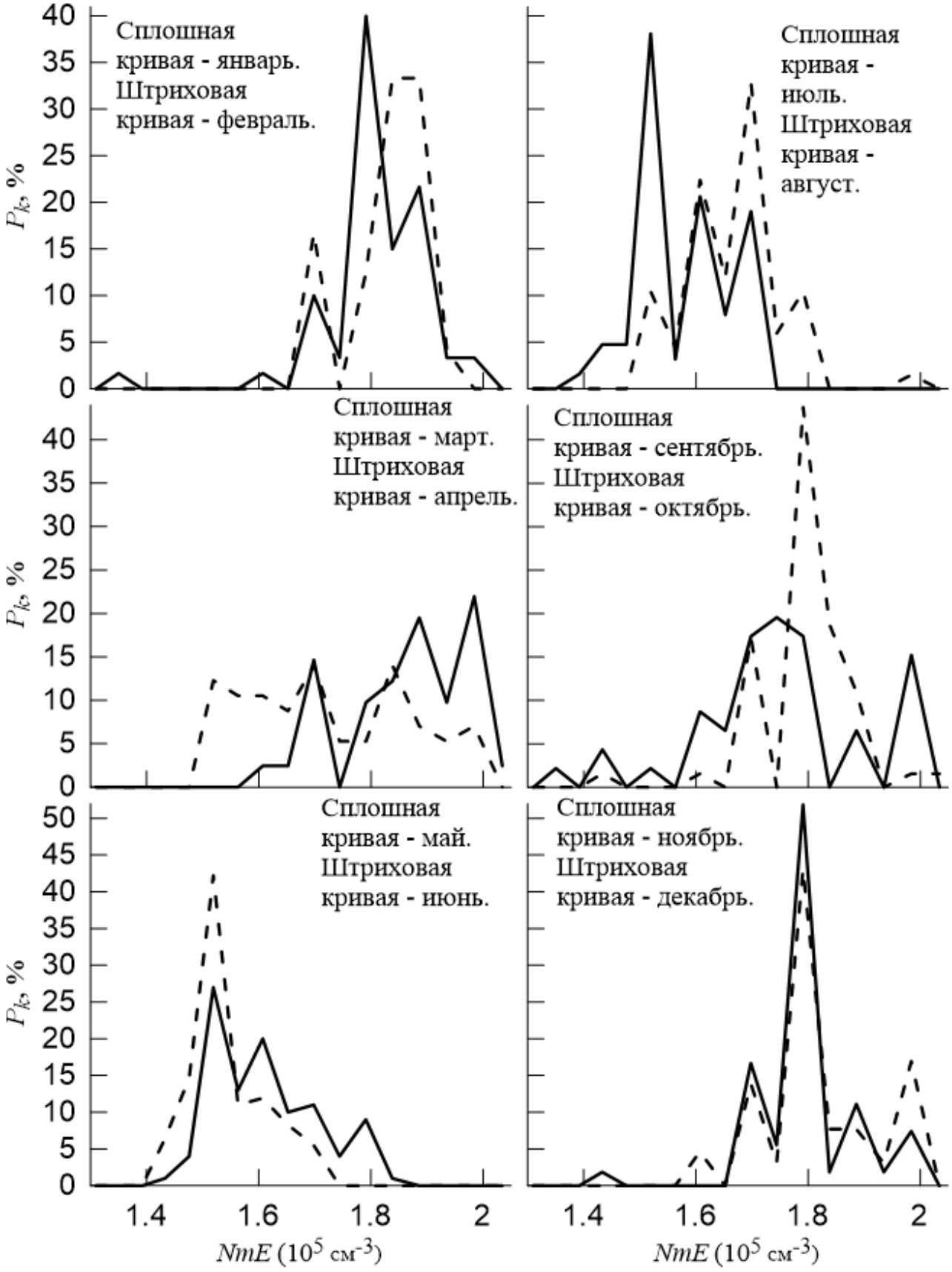
Сплошная кривая - январь. Штриховая кривая - февраль.
Сплошная кривая - июль. Штриховая кривая - август.
Сплошная кривая - март. Штриховая кривая - апрель.
Сплошная кривая - сентябрь. Штриховая кривая - октябрь.
Сплошная кривая - май. Штриховая кривая - июнь.
Сплошная кривая - ноябрь. Штриховая кривая - декабрь.
P_k, %
NmE (10^5 см$^{-3}$)

Figure 2

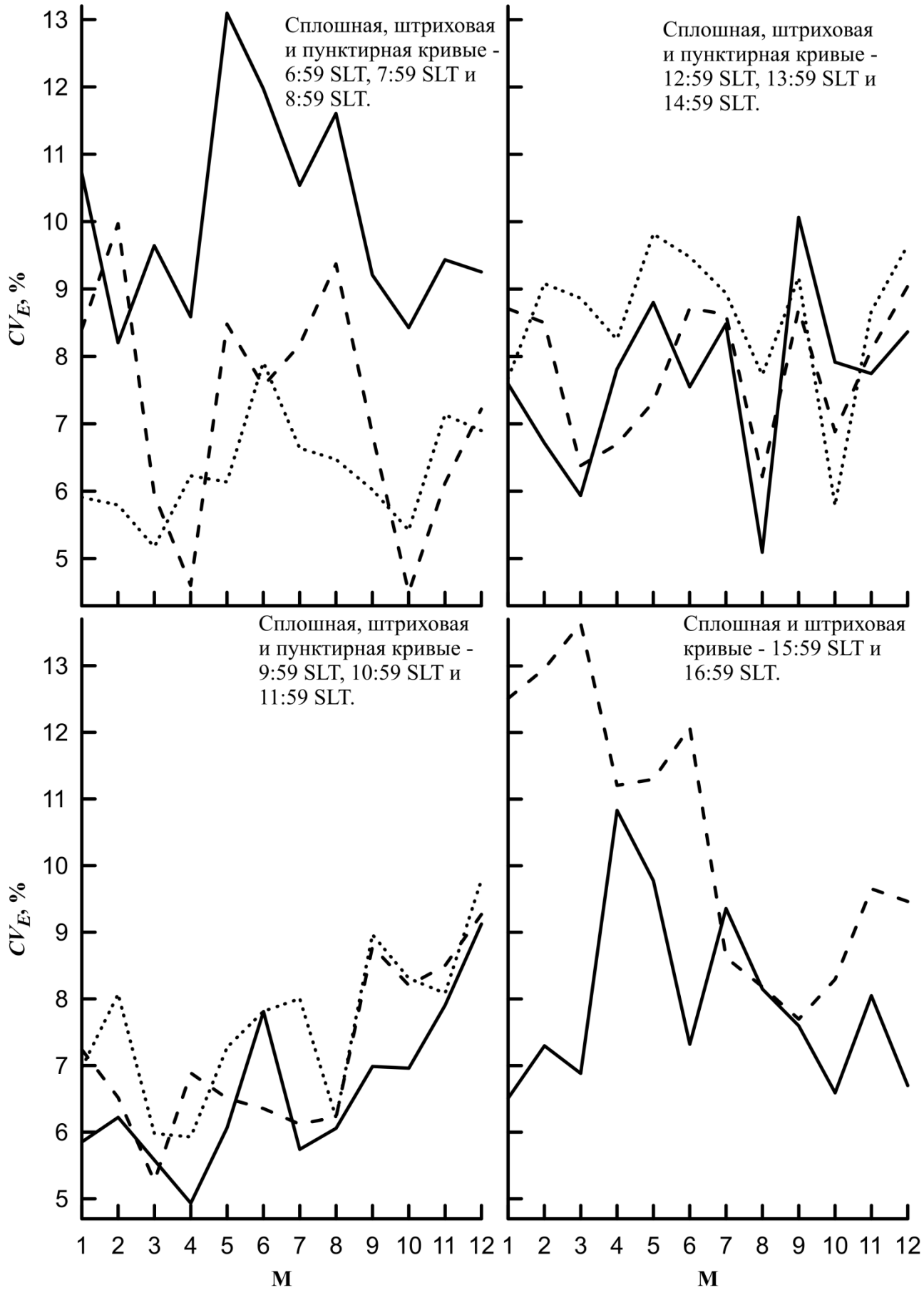
Сплошная, штриховая и пунктирная кривые - 6:59 SLT, 7:59 SLT и 8:59 SLT.
Сплошная, штриховая и пунктирная кривые - 12:59 SLT, 13:59 SLT и 14:59 SLT.
Сплошная, штриховая и пунктирная кривые - 9:59 SLT, 10:59 SLT и 11:59 SLT.
Сплошная и штриховая кривые - 15:59 SLT и 16:59 SLT.
CV_E, %
M

Figure 3.

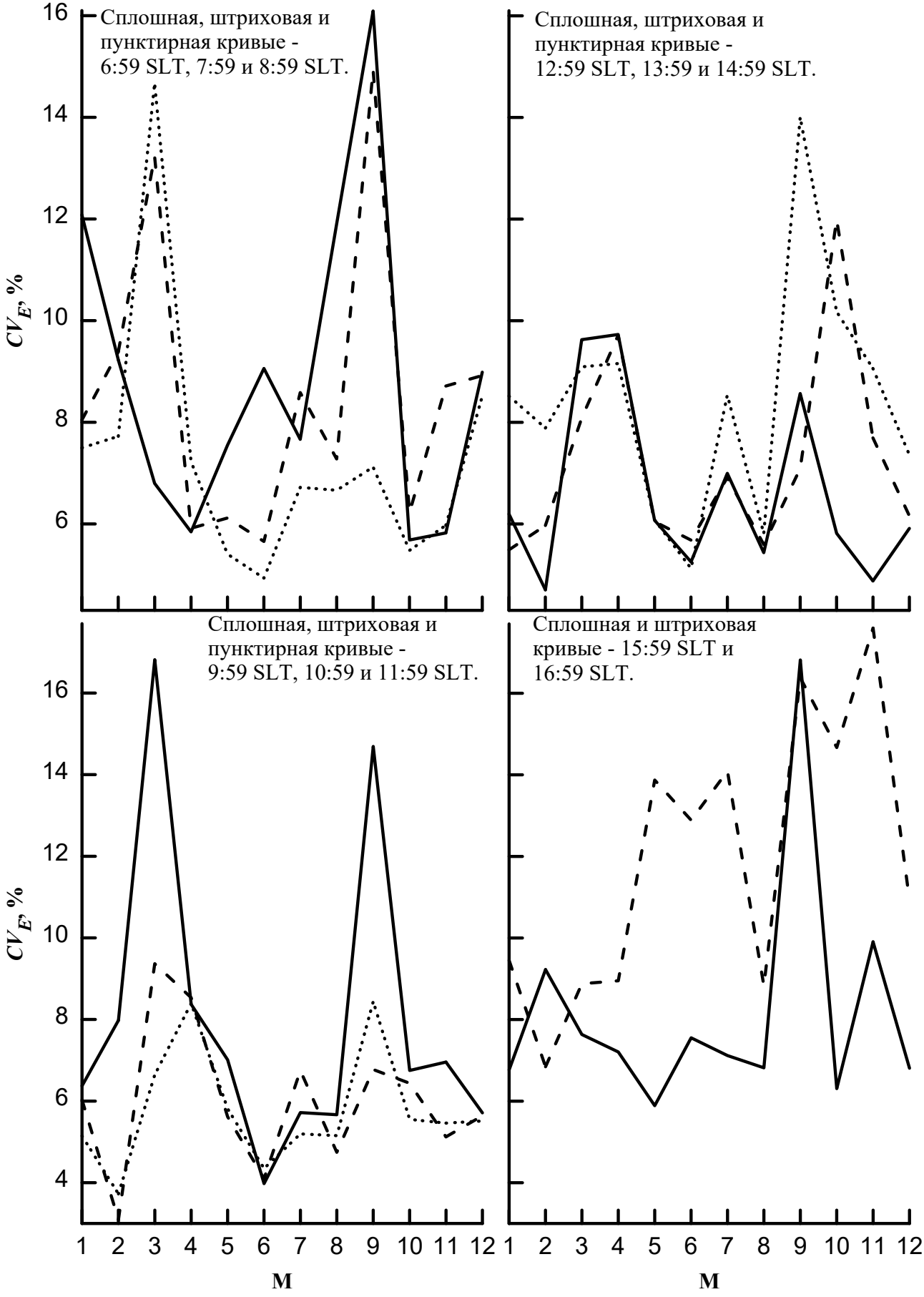
Сплошная, штриховая и
пунктирная кривые -
6:59 SLT, 7:59 и 8:59 SLT.
Сплошная, штриховая и
пунктирная кривые -
12:59 SLT, 13:59 и 14:59 SLT.
Сплошная, штриховая и
пунктирная кривые -
9:59 SLT, 10:59 и 11:59 SLT.
Сплошная и штриховая
кривые - 15:59 SLT и
16:59 SLT.
CV_E, %
M

Figure 4

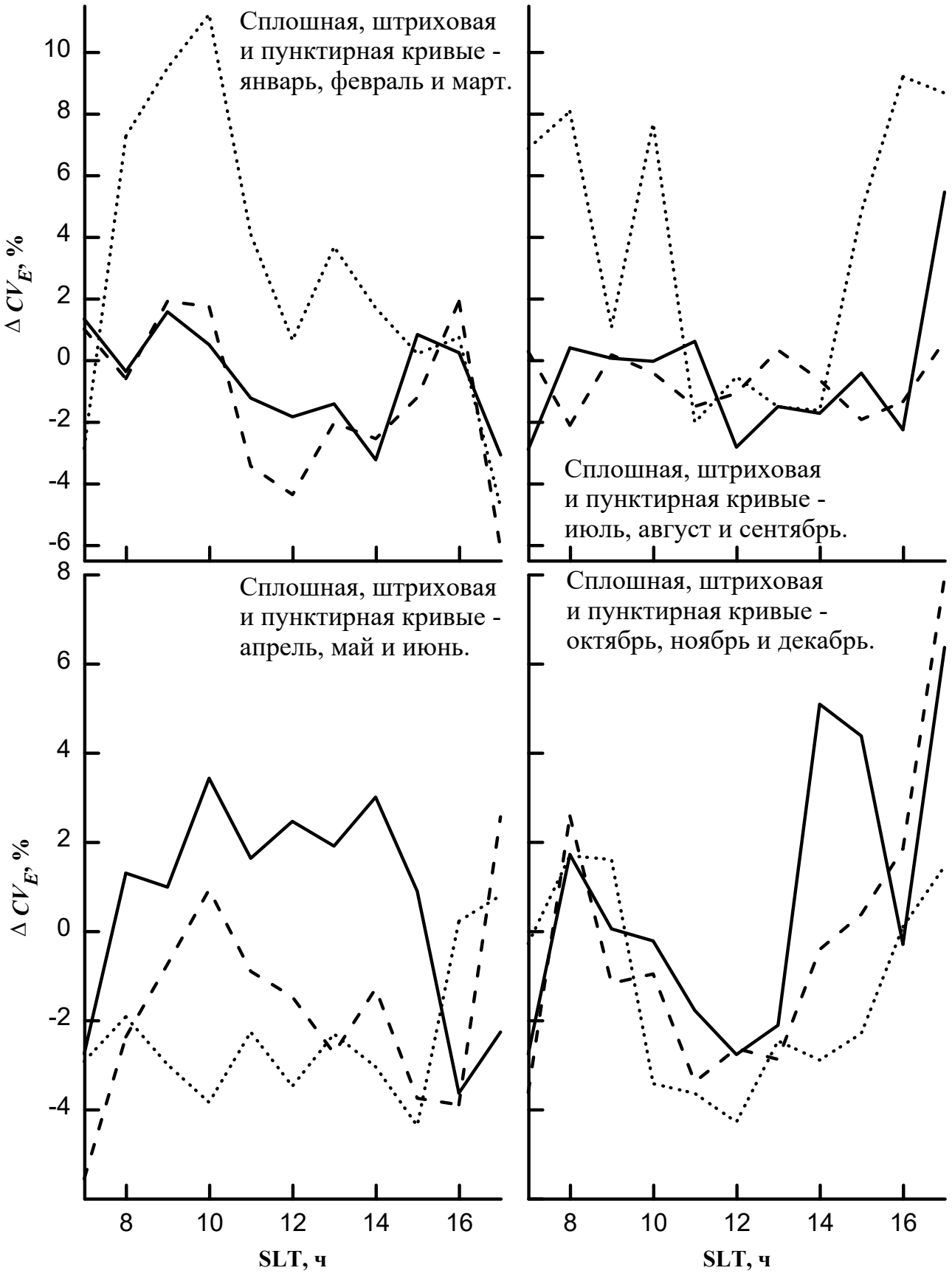
Сплошная, штриховая
и пунктирная кривые -
январь, февраль и март.
Сплошная, штриховая
и пунктирная кривые -
июль, август и сентябрь.
Сплошная, штриховая
и пунктирная кривые -
апрель, май и июнь.
Сплошная, штриховая
и пунктирная кривые -
октябрь, ноябрь и декабрь.
Δ CV_E, %
SLT, ч

Figure 5.

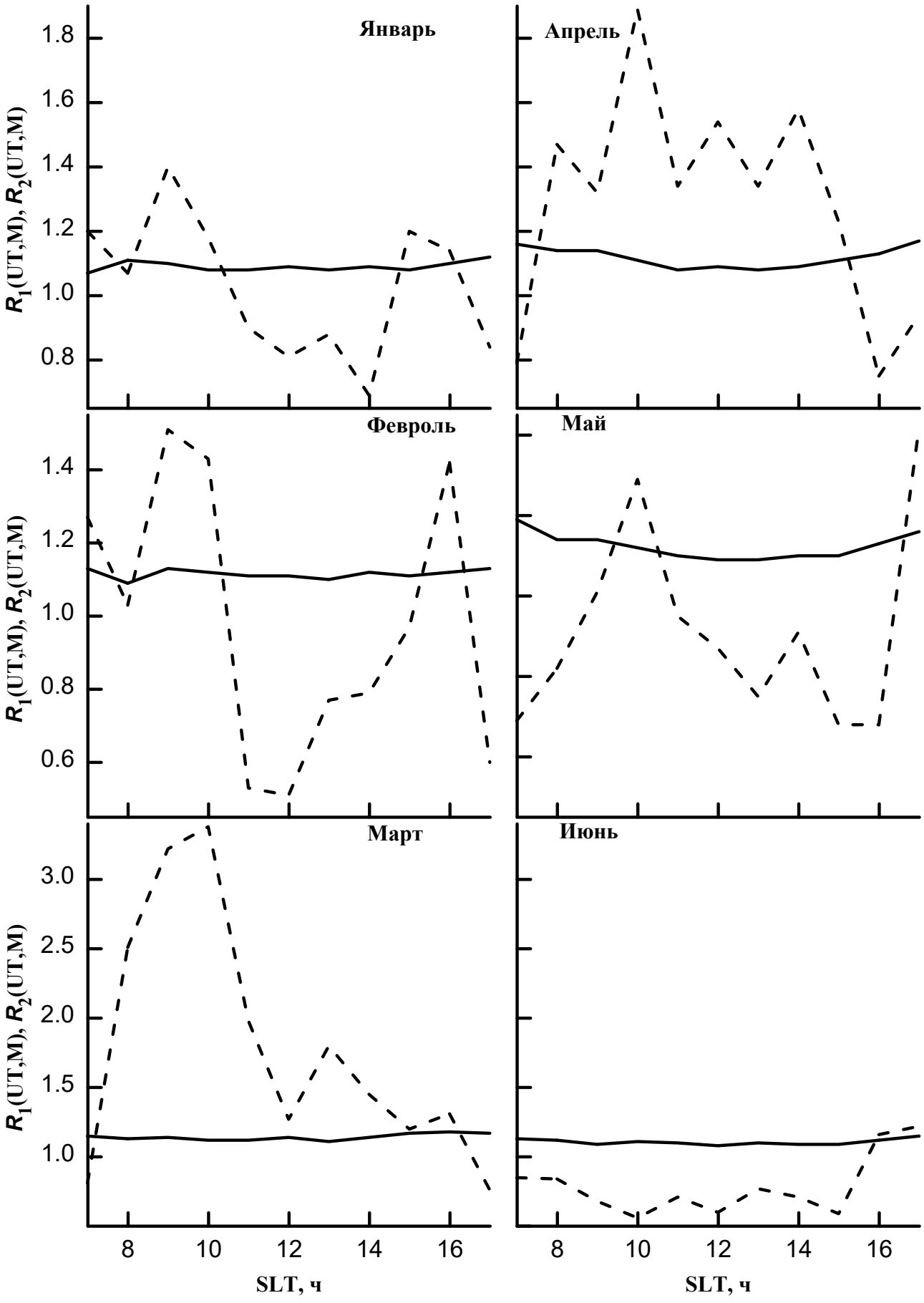

Figure 6

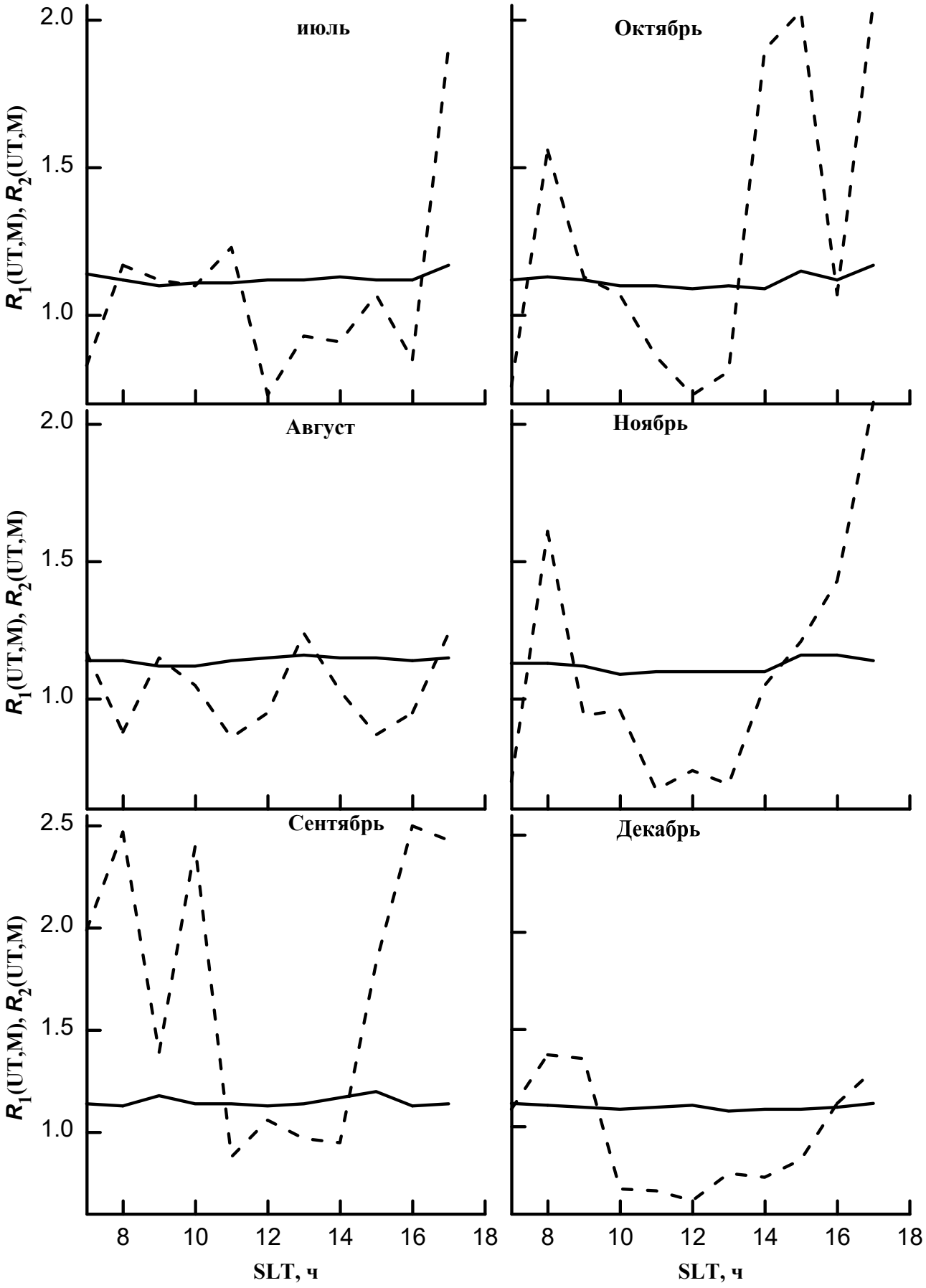
июль
Октябрь
Август
Ноябрь
Сентябрь
Декабрь
R_1(UT,M), R_2(UT,M)
SLT, ч
2.0
1.5
1.0
2.5
8
10
12
14
16
18

Figure 7